

Development of Portable Friction Stir Welding Equipment for In-Space Manufacturing



Peng Li , Wei Zhong, Lijie Guo, Jialiang Zhang, Xiaosong Feng, Fei Li, and Weigang Zhao

Abstract Friction stir welding (FSW) technology is a solid-phase joining process with a non-melting pool in the connection area and insensitivity to gravity, so that it is suitable for construction of the structures in space. However, there is still a large gap between the process of FSW in space and on ground. Conventional on-ground FSW process needs large welding forces and power. Besides, the machines are also very bulky. By comparison, the FSW device in space bears the features of light weight, flexibility, portability, and quickly being in-site. To realize the application of space manufacture, the miniaturization and lowering of energy consumption of FSW equipment adapted to space environment are the key issues which need to be solved. Based on the principle of non-tool-tilt friction stir welding (NTFSW), the realization of lightweight FSW equipment has been put forward, and the mechanical mechanism and the structures of portable FSW device have been designed. The key components of the force-amplifying bionic mechanism—the force-amplifying linkage rod (FALR) modeled on masticating jaw bones and the frame modeled on upper jaws or heads—have been designed and optimized with abundant strength and

P. Li (✉)

School of Materials Science and Engineering, Shanghai Jiao Tong University, Shanghai 200240, China

e-mail: lipeng314159@126.com

P. Li · L. Guo · X. Feng · W. Zhao

Shanghai Aerospace Equipment Manufacturer Co Ltd., Shanghai, China

e-mail: guolijie149@163.com

W. Zhong

Aerospace System Engineering Shanghai, Shanghai, China

e-mail: zhongwei6685@163.com

J. Zhang

School of Mechanical Engineering, Donghua University, Shanghai, China

e-mail: zjili@dhu.edu.cn

F. Li

Shanghai Key Laboratory for High Temperature Materials and Precision Forming, Shanghai Jiao Tong University, Shanghai, China

e-mail: lifei74@sjtu.edu.cn

stiffness. The novel FSW device, with mass weight of 41.75 kg and less than 2.7Kw power, is newly patented, which effectively meets the limitations of design goals and ensures the friction stir additive manufacturing system.

Keywords Non-tool-tilt friction stir welding equipment · Biological modeling design · Design · analysis · and evaluation · Portable · Manufacture in space · Repair on-site

1 Introduction

Friction stir welding (**FSW**) technology, originated in the 1990s, from the welding institute **TWI** in Britain, is newly invented by Thomas et al. [1, 2]. As an advanced solid-phase joining technology, it provides a high-performance and high-quality-stability joining method for the processing of materials which are difficult to be welded by melting-phase joining technology. **FSW** has already been able to weld materials, such as aluminum alloys, magnesium alloys, titanium, high-strength steels, and composite materials. It plays an important connecting and assembling role in the manufacture of rockets, airplanes, high-speed trains, and automobiles [3–5]. In particular, in welding aluminum alloy in the field of aerospace, it overcomes the frequent defects existing in traditional material melting welding, such as crack, slag, and porosity, thus making it possible for manufacturing components of rockets and other high-performance aero-products [6–8]. **FSW** will surely be expanded to more product application fields in the future.

FSW was originally implemented by milling machines. Compared with the structure of the gantry machine version and the parallel machine version [9–11], the **FSW** equipment of milling machine version possesses the advantages of simple structures and easy production, so it is still the most popular general structure. Non-tool-tilt friction stir welding (**NTTFSW**) can be implemented directly by milling machines, but the stirring tools of zero-angle may result in substantial defects in welding seams, such as tunnel defects [12]. Therefore, the parameters of the stirring tool of **FSW**, such as the stirring needle thread, the stirring needle angle, and the stirring shoulder, are also needed to be matched with **NTTFSW**.

The conventional **FSW** equipment is often bulky and heavy, which occupies more jigs and fixtures during the welding process. It is difficult to be handheld flexibly and be used to manufacture the components of large-scale products at speed, thus dissatisfying the requirements of mobile scenarios, including the artificial handheld scenarios and the robot handheld ones. In the fields of maintenance and manufacture of large-scale products, it has become a key problem to provide a flexible and portable **FSW** device that can be quickly put into practice of repairing the space station in space [13], manufacturing devices by **FSW** underwater [14] and so on.

Besides in the field of welding, the friction stirring used for manufacturing materials additively, which can be named as the friction stirring additively manufacturing (**FSAM**), is just in its early stage, but it has gained a considerable value of rapidly

manufacturing the large-scale components. The **FSAM**, with the characteristic of solid-state processing, has become an important development direction of the friction stir technology and has tried to be commercialized—for instance, the Meld Manufacturing Corporation uses the patented **MELD** processing to add new materials by FSW to form parts layer by layer [15, 16].

In order to further expand the **FSW** technology to the fields of welding in special environments and to the additive manufacturing processes, more open, light, and modular **FSW** mechanism are needed; therefore, it is necessary to develop a convenient **FSW** device or equipment.

Based on **NTTFSW**, this study develops a Chinese patent [17] of novel portable **FSW** device, whose structure design, analysis, and finite element calculation are shown in this paper, which aims at advancing the research used in field of the manufacturing by **FSW** device in space. The rest of this paper is organized as follows: the basic principles of **FSW** are analyzed based on design points in Sects. 2 and 3, the design results of the novel portable **FSW** equipment are given, including the system design, functional realization, and the detailed capability of the mechanism; in Sect. 4, the key components of the novel portable **FSW** device are analyzed and optimized by finite element analysis method, in order to ensure both strength and stiffness of the axial force amplifier rod and the frame; Sect. 5 is the conclusion of the paper.

2 Basic Physical Processes and Key Points

2.1 Basic Principles of the Processes

The basic principle of **FSW** technology, depicted in Fig. 1, is to use a tool made by the material which is harder than that in the welded workpieces. Set with a stirring shoulder in larger diameter and a stirring needle in smaller diameter, this tool is a multi-diameter shaft, which keeps rotating friction materials to produce mechanical and thermal energy input, and which travels with the stirring tool rotating to form the force and geometry constraint along the surface of workpieces. By adjusting the rotating frequency and travel velocity of the tool, a heating controllable connection can be formed in the workpieces. Furthermore, with the rotating friction between the stirring tool and the workpieces materials, the technology makes a certain temperature distribution in the connection area in the workpieces. The plasticized flow of the materials of the connected workpieces is generated by the travel and relative rotation of the stirring tool. Finally, a solid-phase diffusion and a state of dispersion welding between the materials of the workpieces are generated.

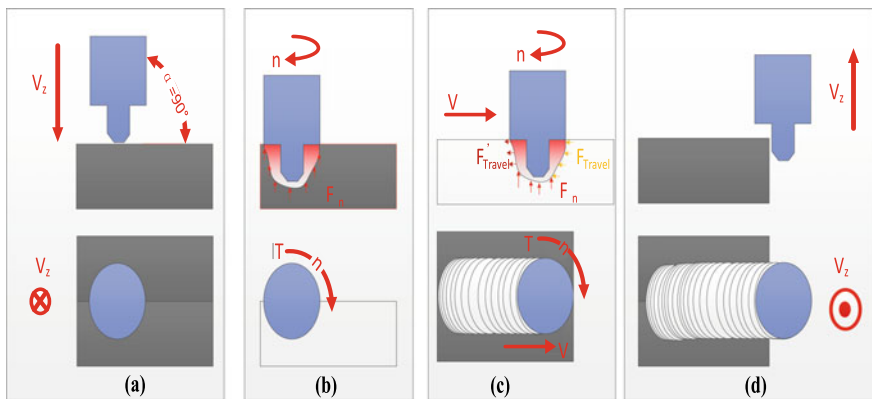
The key to achieving optimum of material microstructure and mechanical performance in the connection area of workpieces depends on the optimal match between the travel velocity V of the stirring tool and the relative rotating speed n of the stirring tool. It is a highly precise and quality-controlled method of solidified connection of

the materials in the workpieces, which is energy-saving, for the controllable temperature gradient generated in the condition of spatiotemporal field of “scanning” the area by the stirring tool. This high degree of precision and easy control of the energy feed are rooted in the energy input by the stirring tool, which has an approximate linear correlation with the welding rotation frequency $f = n/(2\pi)$ and the motion speed V , thus making it easy to grasp the energy feed. Additionally, the joining process involves the superposition of both regular rotational motion and linear motion, by which the motion of the parts’ geometry can also be precisely controlled.

In order to design the FSW equipment, it is a must to carefully analyze the force condition of the stirring tool in each stage of the friction stir process. The FSW process can generally be divided into four stages as depicted in Fig. 1, according to which more details are introduced and analyzed as follows:

(a and b) **From the stirring tool starting to locate the connection track line to the workpieces being touched by the tool, the first stage (a) lasts for an extremely short action time, which belongs to the instantaneous starting stage of the equipment. In the second stage (b), the friction-stirring tool is rotated into the workpieces; meanwhile, the friction begins to generate a thermal field, simultaneously generating the softening and the plasticizing flows of the materials.**

In the first and second stages, the force of the stirring tool depends on the resistance from the workpieces to the stirring tool, which is generated when the stirring tool is rotated and pressed into the workpieces. This resistance Includes: (i) a force of rotating tangential friction, that is, the resistance opposite to the direction of the rotation torque; (ii) an axial force of the stirring tool, that is, the resistance opposite



F_n : The axial force of the stirring tool, that is, the resistance opposite to the downward pressure, et al.; T : Torque of rotating tangential friction; V_z : Velocity close to/remove from the workpiece.; V : Travel velocity; F_{Travel} : Radial force of stirring tool caused by travel; F'_{Travel} : Additional radial force caused by rotation, et al.; $f=n/(2\pi)$; f , the rotating frequency, and n , the rotating speed.; $\theta=(90^\circ-\alpha)$: Angle of the stirring tool-tilt.

Fig. 1 The procedure of Non-tool-tilt friction stir welding

to the downward pressure; (iii) an additional radial force, which is caused by the force of rotor jitter at the moment of starting acceleration, the centrifugal effect of the materials with a certain scale of rotating flow generated by the stirring tool, and other unbalanced states.

- (iii) **In the third stage, the stirring tool continues rotating while scanning the connection track between the pair of workpieces, during which a joint is formed by the progressive contact between the stirring tool in the connection area and the gradual cover of the new solid-phase connection area.**

In the third stage, the force of the stirring tool is subject to the material resistance forces both of the progressive contact of the stirring tool in the area to be connected and of the gradual separation in the new solid-phase connection area. These material resistance forces include: (i) rotating friction torque; (ii) axial force of the stirring tool and (iii) radial force of the stirring tool. At this stage, the force of the stirring tool is generally stable. For example, the source of the force wave is mainly caused by the geometric fluctuations, derived from the structural splicing and trajectory, and the homogeneity of the material microstructure.

- (iv) **In the fourth stage, the joint is completed with the completion of the scanning of the connection track line and the withdrawal of the stirring tool from the workpiece materials.**

In the fourth stage, the withdrawal force of the stirring tool is mainly influenced by the spatial distribution of the materials and the force fluctuations in the local scale area.

2.2 Design Consideration on Practical Application

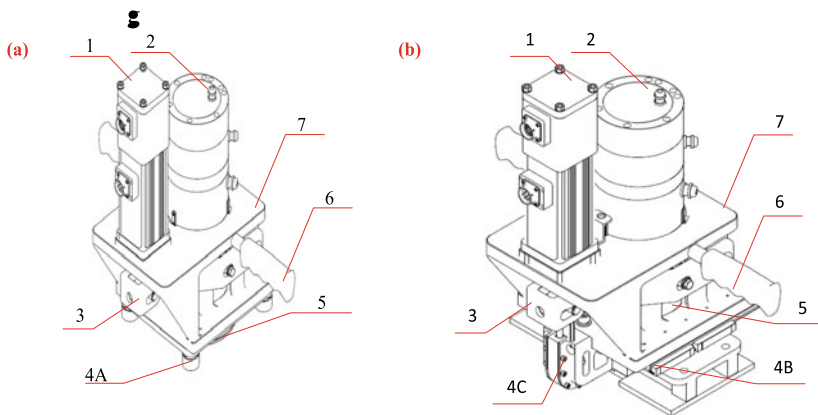
Based on the process analysis of the basic principles above, it is easy to deduce that the axial force, the radial force, and the torque of the stirring tool, fluctuating in a relatively high frequency, present a working condition with the combination of “Pressure-Bend-Twist”. During the FSW process, the task is to achieve a good welding joint mainly through the method of controlling the axial displacement or/and the press force size of the stirring tool. This research is designed based on the hand-held structure, a Chinese patent [17], whose major application scenario is on-site repair. The modular device of this patent can also be embedded to compound with other machine tools. Considering the need for on-site repair, the requirements and difficulties of designing the FSW equipment are listed as follows: (a) the weight of the equipment should be as light as possible, with the mass ≤ 60 kg and the power no higher than 2.7Kw, so that it has the capability to weld the aluminum alloys in the maximum thickness of 6 mm; (b) its configuration should be convenient for hand-holding or hand-guiding by designing a feeding force-amplifying mechanism within the scope of Ergonomics; (c) the forces applied to the reciprocity area of the tool and

the materials should satisfy the process, with a maximum axial force >15000 N and a maximum radial force >5000 N [18]; (d) the stiffness of the structure should be large enough to avoid FSW force fluctuations which will affect the handheld effect, and the strength and the stiffness of the key components should be optimized through analysis and calculation.

3 Results of the Design and Its Development

3.1 General Design of FSW Equipment

The novel FSW equipment, as shown in Fig. 2, is consisted of a traveling system, maintained by a handle, for resisting the radial force, a stirring tool feeding system for axially putting and withdrawing the stirring tool into and from the workpieces, a rotating system with the compact motorized electrical spindle for ensuring the friction thermal of weld under the assistance of the stirring tool, and an axial feeding force-amplifying system (AFFAS), driven by an electrical cylinder, for producing a greater axial force, thus helping implement the axial feeding and the axial driving to the spindle and the stirring tool.



1: Electrical cylinder with roller screws of axial feeding system; 2: Compact motorized electrical spindle of rotating system; 3: Force amplifying linkage rod (*The masticated jaw bone*); 4A: Rolling foot of chassis of travelling driver system; 4B: Rolling guide of chassis of travelling driver system; 4C: Commutator for axial feeding force to travelling force; 5: Mounting end of the stirring tool; 6: handle for manual pushing and pressing; 7: Frame (*The upper jaw and head*).

Fig. 2 Schematic diagram of overall design and walking scheme: **a** Large range of hand push (including manipulator), the left; **b** Small range of machine self-feeding, the right

3.1.1 Traveling Driver System

The traveling system of the novel **FSW** equipment realizes the “scanning” of the welding track of the friction-stirring welding. The equipment is supposed to have two modes—manual pushing and automatic walking [17], and two functions—NTTFSW and friction stir pull/plug welding. As shown in Fig. 2, the differences between the two modes lie in the chassis of the traveling system: Fig. 2a is the type of four rolling feet, while Fig. 2b is the type of two rolling guides. If the welded plate is thin, the offset of the forging force, which is equivalent to the axial force, and the torque can be achieved just by hand pressing. If the welded plate is thick, two rolling guide rails should be laid along the welded parts, and a commutator should be applied to offset the forward resistance, which is the radial force, and the torque.

3.1.2 Axial Feeding System and Driver

According to the principles of the process, an axial feeding system is needed for **FSW** to realize the pressing and withdrawal of the stirring tool. The key components of the **AFFAS** are the force-amplifying linkage rod (**FALR**), an important transmitting and moving part, and the frame, the foundation of fixation and mounting. Considering that the handheld **FSW** equipment in this study has a high structural effectiveness in terms of mechanism function and structure safety, the design is carried out by using the force-amplifying linkage system, which is enlightened by the biological mechanism of animal mouths.

In order to achieve light weight and large application force, an electrical cylinder with roller screws is adopted to drive the linear motion and to make power source of the precise axial feeding system [19]. The servo electric cylinder, **GSX30**, of Lim-Tec Corporation is adopted. It is 4.3 **kg** in weight, which can output the $F_e = 5620$ N external push/pull force, the $H = 75$ mm motion stroke, and the $V = 127$ mm/s maximum speed. The linear accuracy of **GSX30** is 0.025 mm/300 mm. Considering that the motion stroke of the electric cylinder of this equipment is $H = 75$ mm and the error estimate of the screw bearing in the cylinder is calculated by accumulation, the stiffness of the electric cylinder is 0.00625 mm/75 mm.

3.1.3 Rotational Spindle Driver

A compact motorized electrical spindle [18], adopted in the rotating system, is also specially customized with a rated speed $n = 3500$ rpm, a maximum speed $n_{max} = 8000$ rpm, a maximum axial force $F_n > 15000$ N, and a maximum radial force $F_r > 5000$ N. The requirements of light weight, high speed, high torque, and large load can be achieved through customized design. For example, in order to realize weight reduction, the spindle shell is partially made by aluminum alloy and the core shaft is made of high-strength steel.

3.2 Implement Results of FSW Equipment

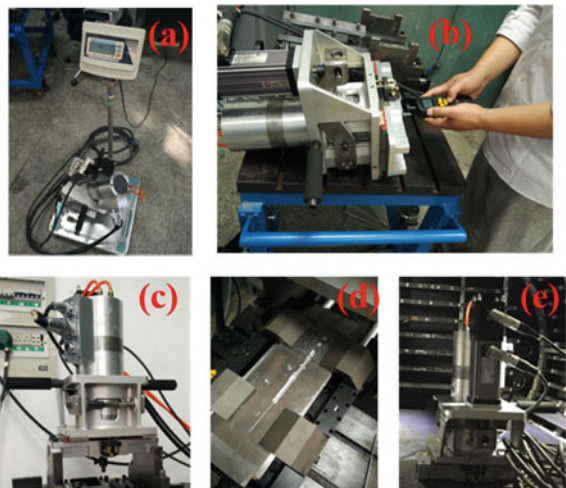
According to the design and the development introduced above, the implement results of the handheld FSW equipment are shown in Fig. 3. As in Fig. 3a, the weight of FSW equipment was reduced from 52 to 41.75 kg, that is, the weight loss rate reaches about 20%. Figure 3b and c demonstrate the routine testing. The conventional test of welding seam is shown in Fig. 3d, which proves that it can weld the Aluminum Alloy 5A06 with the maximum thickness of 6 mm. Figure 3e shows the temperature environmental test which emulates the working condition in space. The results have been verified to be consistent with design objectives; therefore, the equipment is expected to be used in future space manufacturing scenarios, such as the forming, joining, and repairing processes of the in-orbit structure of the space station.

4 Analysis and Evaluation of the Key Designs

4.1 Axial Feeding Force Amplifying Mechanism (AFFAM)

As mentioned before, the key parts of the new portable FSW equipment are the FALR and the frame. In this study, the design of the FALR is ideally similar to the structure of masticated jaw bones, which must maintain a certain strength and stiffness to ensure the precise control of the pressing distance on the stirring shoulder. The frame is similar to the structure of upper jaws and heads, which exerts the reaction forces, bears the large loads, and also holds and provides mounting interfaces and a platform for other parts.

Fig. 3 Verify portable FSW equipment: **a** The test of weight; **b** The test of working rotating speeds; **c** The welding test status on ground; **d** The welding seam; **e** Simulation space state test



In the process of biological evolution, it is significant for heads and jaws to adapt to the environment. In order to provide more evolving space for other organs, strong feeding and chewing system should be developed with light and well-distributed weight. The head and jaw structures of typical creatures are shown in Fig. 4 [20]. The head of *ceratosaurus nasicornis* who is a 6-m sized heavyweight meat-eater of the Jurassic [20] is shown on the left of Fig. 4. Large food intake is presumably achieved by a strong maxillary skull and a mandibular arch and driven by strong lip muscles.

Unlike heavyweight land animals, fish are unable to get enough reaction forces of chewing, tearing, and other activities from grasping the ground, which leads to the evolution of the mechanism with more complicated structures and the weight loss to a larger extent. The typical fish mouth mechanism of haddock *melanogrammus aeglefinus* is shown on the right of Fig. 4 [20]. Fish have evolved a more lightweight mechanism, for the reaction force of water is obviously weaker. In fact, due to the buoyancy effect of fish bladders and other parts, the activities of fish in deep water have similar characteristics of weightlessness, which can be basically equivalent to the mechanical condition of manufacture in space far away from the ground.

The bionically designed **AFFAM** is a hybrid mechanism. As shown in Fig. 5, the serial mechanism of **AFFAM** contains the degree of freedom (**H**) of the electric cylinder movement, and the degree of freedom (**b**) of rs_3 , which is related to the rolling and sliding motion. The parallel mechanism adopts two-stage parallel topology: the first stage consists of a degree of freedom of the rolling and sliding pairs (**rs1**, **rs2**) and a degree of freedom of the rotating pairs (**r1**, **r2**); the second stage is the degree of freedom (**h**) of the moving pairs (**s1**, **s2**, **s3**), which belong to the motorized electrical spindle. The adoption of multistage parallel topology is beneficial to the realization of the stiffness of the overall structure and to the alleviation of the influence of wave dynamics of the welding parts on the handheld effect.

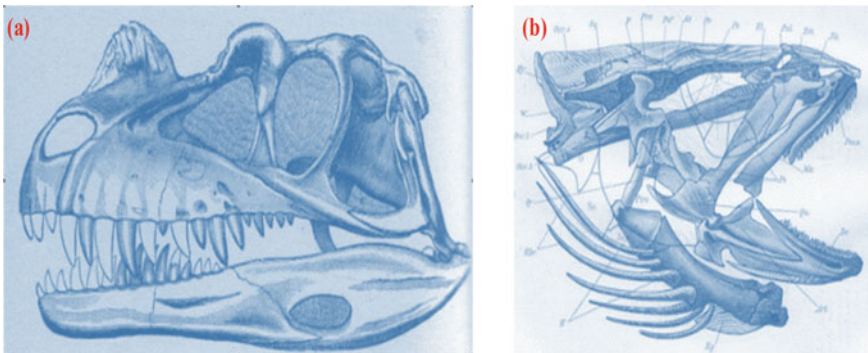


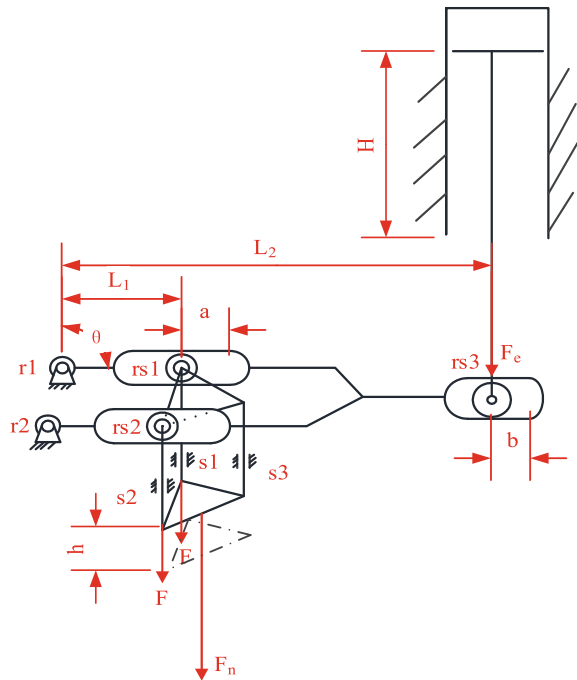
Fig. 4 the head and jaw structure: **a** *ceratosaurus nasicornis* (6-m-sized heavyweight meat-eater of the Jurassic), the left; **b** the haddock *melanogrammus aeglefinus*, the right; reprinted from Ref. [20], copyright 2007, with permission from Springer Science + Business Media, LLC

The output of the electric cylinder is the push/pull force F_e , whose maximum stroke is H . The axial force F_n of the motorized spindle output-end is applied to the stirring tool. The maximum stroke of the up and down movement of the motorized spindle is H . What's more, F is the force on the single ear seat of the motorized spindle, whose maximum linear stroke along the **FALR** is a , while the maximum linear stroke along the **FALR** of the output roller pair of the electric cylinder is b .

Referring to the lever principle, the mechanism above is designed to axially drive the motorized spindle up and down by applying force to the rolling and sliding pairs (**rs1**, **rs2**), which are constituted by the two-ear-blocks of the motorized spindle and the double-forks of the **FALR** modeled on the masticated jaw bones. The double-forks of the **FALR** are connected to the frame modeled after the upper jaw and head through the rotating pairs (**r1**, **r2**). The head and the output shaft of the electric cylinder constitute the rolling and sliding pair **rs3**. The motorized spindle is connected to the frame by three sliding pairs (**s1**, **s2**, **s3**), enabling the motorized spindle to move up and down and to transmit torque to the frame.

By analyzing the schematic diagram of the mechanism in Fig. 5, the transmission ratio of the **AFFAM** is $L2: L1$. Based on the maximum push/pull force $F_e = 5620$ N of the electric cylinder, the **AFFAM** with a transmission ratio of 3 is selected, that is, the ratio of $L2: L1 = 3$, so that the spindle is able to reach up to no less than 15000 N push/pull force, for the push/pull force of the spindle end is 3 times the quantity of that of the electric cylinder. When controlling the **AFFAM**, either the constant-force

Fig. 5 Schematic diagram of the mechanism of the axial feed scheme



mode of the electric cylinder push/pull or the constant-output-speed mode of the electric cylinder push/pull can be adopted. Due to the conservation of instantaneous power of the mechanism, the travel stroke, the speed, and the force of the motorized spindle are proportional to the transmission ratio of the **AFFAM**. After conversion, the force applied to the motorized spindle is proportional to $F_n = 3 * F_e = 16860 \text{ N}$, the motion stroke of the motorized spindle is inversely proportional to $h = H/3 = 25 \text{ mm}$, and the maximum speed of the motorized spindle is inversely proportional to $v = V/3 = 42.3 \text{ mm/s}$.

4.2 Strength and Stiffness Analysis of the **FALR**

4.2.1 Methodology and Design

According to the force analysis of **FSW** at each stage in Sect. 2.1, the **FALR** demonstrates a series of mechanical behaviors, and the axial stiffness of the end of the stirring tool is required to be no more than 0.5 mm/25 mm regarding to the process analysis. Additionally, considering the design that the axial force-amplifying ratio is 3, the axial stiffness of the output shaft of the electric cylinder is required to be less than 1.5 mm/75 mm. Finally, all key components become adequately lightweight and reasonable in structure after optimization.

The software is used in the design to establish a three-dimensional model of the **FALR** which is shown in Fig. 6a. The material used in the **FALR** is **40Cr**, whose mechanical properties are shown in Table 1.

The software **ANSYS 12.0.1** is used for finite element modeling of the **FALR**. In order to improve the optimizing efficiency of the design, tetrahedral mesh is used, in

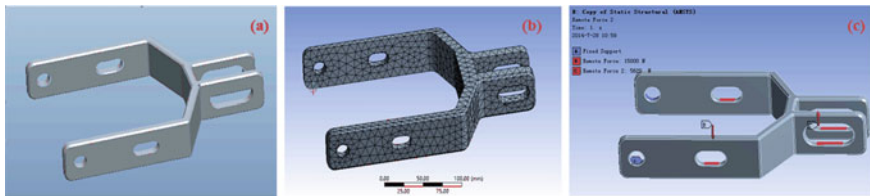


Fig. 6 Design and **FEA** modeling of the force-amplifying linkage rod (The masticated jaw bone): **a** The part model, the left; **b** The meshing, in the center; **c** Constraints and the working force conditions, the right

Table 1 Mechanical properties of alloy steel **40Cr**

Yield strength	Fracture strength	Modulus of elasticity	Poisson's ratio	Micro hardness
790 MPa	984 MPa	210 GPa	0.29	301 HV

which the number of nodes and cells are 7153 and 3730, respectively. The meshing generated by ANSYS is shown in Fig. 6b.

As shown in Fig. 6c, the forces and constraints of the FALR are established according to its process principles in Sect. 2.1, with reference to the force model of the mechanism in Fig. 5 that a fixed constraint is applied to the rotating pairs (r1, r2) on the left of the FALR in order to simplify the stress state. What's more, concentrated forces $F_n = 15000\text{ N}$ and $F_e = 5620\text{ N}$ are applied on the enveloped track planes, which, respectively, contact the pin holes of the two rolling and sliding pairs (rs1, rs2) in the middle of the FALR and the rolling and sliding pair rs3 at the right head of the FALR. Gravity and inertial forces are ignored.

4.2.2 Results and Analysis

On one hand, as shown in Fig. 7a, the cloud map of the stress distribution in the FALR is obtained by FEA solution. The maximum stress, located at the corner of the FALR, is about 255 MPa, which is suitable for use.

On the other hand, regardless of the motorized spindle deformation, the total deformation, 0.964 mm, including the deformation of the FALR, 0.958 mm, and of the motor cylinder itself, 0.006 mm, is converted to the spindle end stiffness of 0.321 mm/25 mm. The cloud map of the deformation distribution of the FALR in Fig. 7b proves that the maximum deformation of FALR, 0.958 mm, lies in the rolling and sliding pair rs3, on which the electric cylinder acts.

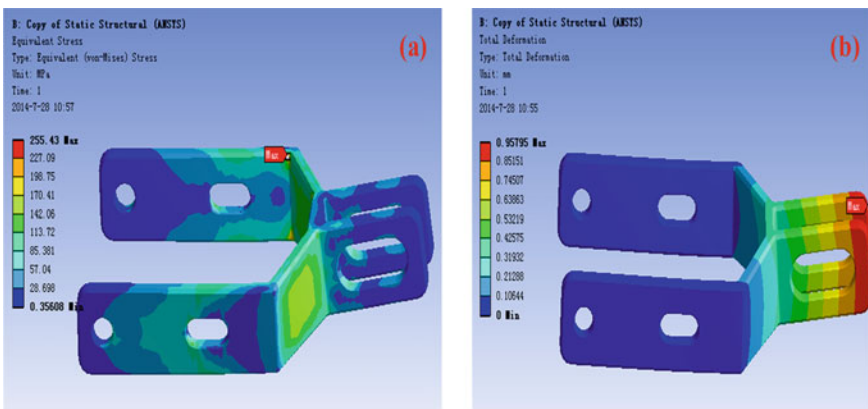


Fig. 7 Preliminary calculation of mechanical behavior of the force-amplifying linkage rod (The masticated jaw bone): a The maximum stress, the left; b The maximum deformation, the right

4.2.3 Effect Evaluation and Suggestions

Based on the statistics above, the maximum stress of the **FALR** is 255 MPa, and the stiffness of the end of the stirring tool is 0.321 mm/25 mm, which does not meet the requirements.

Therefore, in order to enhance the stiffness of the **FALR**, the right head is linked by a block of material; meanwhile, some other geometrical entities are removed appropriately according to the stress distribution to improve the stress path, as shown in Fig. 8a.

The results of the relatively new design of the **FALR** are shown in Fig. 8b and Fig. 8c. The deformation of the new **FALR** at the cashew-nut-shaped pin holes on the right side is less than 0.6 mm, the stiffness of the spindle end is less than 0.2 mm/25 mm, and the new maximum stress is 213 MPa, which are all suitable for use.

4.3 Strength and Stiffness Analysis of the Frame

4.3.1 Methodology and Design

According to the functions of **FSW**, the part model of frame modeled on the upper jaw and head is established, as shown in Fig. 9a. The material of the frame is the forged aluminum **LD10**, which is equal to **AA 2A14**, whose mechanical properties are shown in Table 2.

In order to improve the optimization efficiency, tetrahedral mesh is used in Fig. 9b, with 53,512 nodes and 30,254 cells. Figure 9c shows the load conditions and constraints of the frame. A fixed constraint is applied at the bottom plane, and

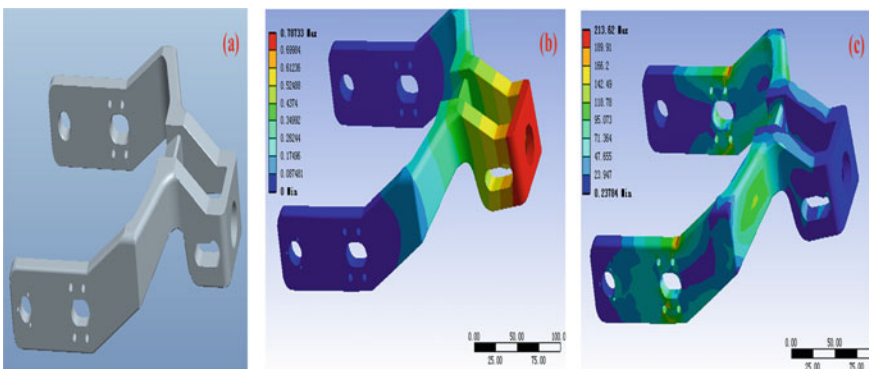


Fig. 8 Optimization and improvement results of the force-amplifying linkage rod (The masticated jaw bone): **a** The improved part model, the right; **b** The ultimate deformation, in the center; **c** Final stress analysis, the right

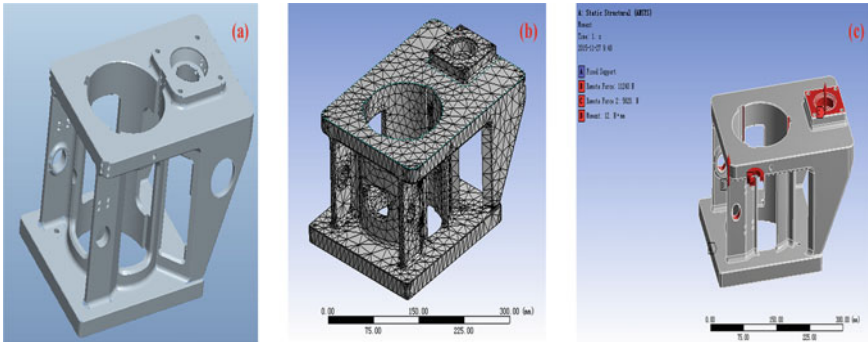


Fig. 9 Design and **FEA** modeling of the Frame (The upper jaw and head): **a** The part model, the left; **b** The meshing, in the center; **c** constraints and force conditions, the right

Table 2 Mechanical properties of forged aluminum **LD10 (2A14)**

Yield strength	Fracture strength	Modulus of elasticity	Poisson’s ratio	Micro hardness
327 MPa	451 MPa	73.1 GPa	0.33	142 HV

a concentrated force of 11240 N is exerted on the mounting hole of the bi-furcation of the **FALR**. A force $F_e = 5620$ N is applied to the mounting hole of the electric cylinder, and a 12Nm torque is applied to the sliding track mounting slot of the spindle. Gravity and inertial forces are ignored.

4.3.2 Results and Analysis

As shown in Fig. 10a, the cloud map of the stress distribution in the frame, with the maximum stress of 48 MPa, is obtained by **FEA** solution. It is shown in the cloud map of the deformation distribution of the frame in Fig. 10b that the maximum deformation, 0.036 mm, is located in the connecting hole of the electric cylinder.

4.3.3 Effect Evaluation and Suggestions

As mentioned above, the maximum strength, 48 MPa, and the maximum deformation, 0.036 mm, are both small enough to meet the demands. The aluminum alloy chosen for the part is adequately lightweight and reasonable in structure, which can be manufactured by five-axis numerical milling machines. Furthermore, the frame can also be designed by topological optimization and be manufactured by additive manufacturing machines, thus achieving a higher degree of lightweight, so that it has the potential to be used in improved versions.

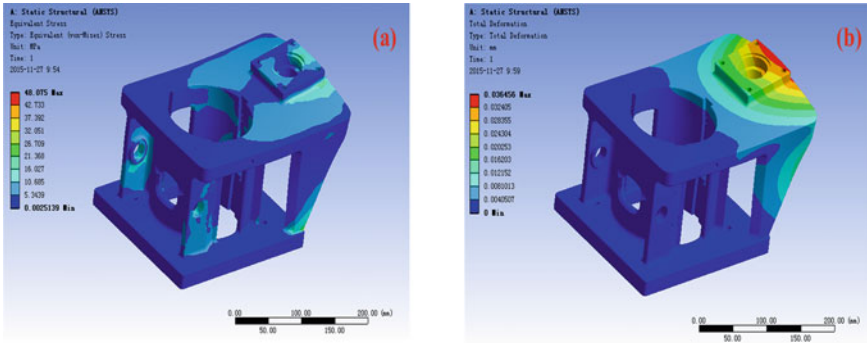


Fig. 10 The computational mechanical behavior of the frame (The upper jaw and head): **a** The maximum stress, the left; **b** The maximum deformation, the right

5 Conclusions

- (1) Based on the analysis of the critical principles of **FSW** and the force-amplifying mechanism inspired by the biological enlightenment of the mechanism of animal mouths, the paper gives a design of a portable **FSW** equipment, which applies the electric cylinder and the motorized spindle, for welding in space in space stations, and analyzes the functional capability of the system and the components in it.
- (2) Through the **FEA** solution, the **FALR** and the frame, modeled, respectively, on the masticated jaw bone and the upper jaw and head, are analyzed and optimized. The improvements are obvious that the weight of the **FSW** equipment is reduced from 52 to 41.75 kg, with the dewatering rate reaching about 20%; besides, it has the capability of welding at most 6-mm-thick aluminum alloys. In line with the research objectives, the **FSW** equipment has been well developed, tested, and validated for operation.
- (3) The **FSW** equipment in this paper provides a very flexible, open, and effective equipment foundation for testing the new technology of **FSW** in space, which can also be suitable for universities and other research facilities to develop freely in new application scenarios, such as in friction stir additive manufacturing, and thus is worth popularization.

Acknowledgements Other efforts about the study described in this paper have also been paid by the following personnel during the years from 2014 to 2015: ZHAO huihui; WEN shanshan; TIAN Hailin; LIU Xinbo; DONG fengbo; WU Rongzong. I would like to extend my heartfelt thanks to them.

This article was written with the help of YAN Xiuyi; ZHANG Jialiang; LI Fei. I would like to extend my heartfelt thanks to them.

The authors also gratefully acknowledge the helpful comments and suggestions of the reviewers, which have improved the presentation.

Contribution of each author **Peng LI:** Methodology, Investigation, Writing—Original draft preparation. **Wei ZHONG:** Validation, Application Background Research. **Lijie GUO:** Funding acquisition, Conceptualization, Supervision Visualization. **Jialiang ZHANG:** Conceptualization, Writing—Reviewing and Editing. **Xiaosong FENG:** Data curation, Resources, Funding acquisition. **Fei LI:** Writing—Reviewing and Editing. **Weigang ZHAO:** Validation and Test.

Term	Definition
Conceptualization	Ideas; formulation or evolution of overarching research goals and aims
Methodology	Development or design of methodology; creation of models
Software	Programming, software development; designing computer programs; implementation of the computer code and supporting algorithms; testing of existing code components
Validation	Verification, whether as a part of the activity or separate, of the overall replication/ reproducibility of results/experiments and other research outputs
Formal analysis	Application of statistical, mathematical, computational, or other formal techniques to analyze or synthesize study data
Investigation	Conducting a research and investigation process, specifically performing the experiments, or data/evidence collection
Resources	Provision of study materials, reagents, materials, patients, laboratory samples, animals, instrumentation, computing resources, or other analysis tools
Data Curation	Management activities to annotate (produce metadata), scrub data and maintain research data (including software code, where it is necessary for interpreting the data itself) for initial use and later reuse
Writing—Original Draft	Preparation, creation and/or presentation of the published work, specifically writing the initial draft (including substantive translation)
Writing—Review and Editing	Preparation, creation and/or presentation of the published work by those from the original research group, specifically critical review, commentary or revision—including pre- or postpublication stages
Visualization	Preparation, creation and/or presentation of the published work, specifically visualization/ data presentation
Supervision	Oversight and leadership responsibility for the research activity planning and execution, including mentorship external to the core team
Project administration	Management and coordination responsibility for the research activity planning and execution
Funding acquisition	Acquisition of the financial support for the project leading to this publication

Data Availability Statements The data that support the findings of this study are available from Shanghai Aerospace Equipment Manufacturer Co., Ltd (SAEM) but restrictions apply to the availability of these data, which were used under license for the current study, and so are not publicly available. Data are however available from the authors upon reasonable request and with permission of SAEM.

References

1. Thomas WM, Nicholas ED (1997) Friction stir welding for the transportation industries. *Mater Design* v18(Nos. 4/6):269–273
2. Thomas WM (1991) Friction stir butt welding. International Patent Application No PCT/GB92 Patent Application, No.9125978.8
3. Gibson BT, Lammlein DH, Prater TJ et al (2014) Friction stir welding: process, automation, and control. *J Manuf Process* v16(1):56–73
4. Mendes N, Neto P, Loureiro A et al (2016) Machines and control systems for friction stir welding: a review. *Mater Design* v90(15):256–265
5. Zeng G, Dong-feng C, Peng W et al (2017) Friction stir welding of packaging container made of SiC_p/Al composites with low volume fraction. *Bulle Chinese Ceramic Soc* v36(05): 1735–1739. <https://doi.org/10.16552/j.cnki.issn1001-1625.2017.05.047>
6. Vairis A, Papazafeiropoulos G, Tsainis A (2016) A comparison between friction stir welding, linear friction welding and rotary friction welding. *Adv Manuf* 4(4):296–304. <https://doi.org/10.1007/s40436-016-0163-4>
7. Boitsov A, Kuritsyn D, Siluyanova M et al (2018) Friction stir welding in the aerospace industry. *Russian Eng Res* v38(12):1029–1033
8. Shtrikman MM, Kornevich AP, Pinskiy AV et al (2018) Friction stir welding of ribbed panels of aircraft airframes. *Weld Int* v32(3):219–222. <https://doi.org/10.1080/09507116.2017.1388048>
9. Teng W, Weizhong G (2019) Modeling and simulation of welding capability for a hybrid friction stir welding equipment. *Mach Design Res* v35(01):175–178
10. Faquan Z, Yongyong L, Ye W et al (2015) Virtual machining function of CNC system for parallel mechanism friction stir welding machine. *Electr Weld Mach* v45(05):6–10
11. Minhong W, Weijia Z, Haitao L et al (2018) Design and motion control of the high precision heavy load friction stir welding robot. *Robot* v40(06):817–824+834. <https://doi.org/10.13973/j.cnki.robot.170560>
12. Ghazanfar B, Awang M, Khan SR et al (2013) Development of a new approach for incorporating tool tilting in friction stir welding. *Adv Mater Res* 701:378–381. <https://doi.org/10.4028/www.scientific.net/amr.701.378>
13. Longhurst WR, Cox CD, Gibson BT et al (2017) Development of friction stir welding technologies for in-space manufacturing. *Int J Adv Manuf Technol* 90:81–91
14. Farzad H, Alireza A, Mohammad A (2017) Effects of processing parameters on microstructure and mechanical behaviors of underwater friction stir welding of Al5083 alloy. *J Manuf Process* v25:77–84. <https://doi.org/10.1016/j.jmapro.2016.11.002>
15. Calvert JB (2015) Microstructure and mechanical properties of WE43 alloy produced via additive friction stir technology. Dissertation, Virginia Polytechnic Institute and State University
16. Hardwick N, Cox C, Schultz JP et al (2018) Meld solid-state joining of different features to cast parts. USA Patent NO.: US20180361501A1
17. Peng L, Chenglin Z, Weigang Z et al (2019) Hand-held du-al-function rotary friction welding device and welding method. Chinese Patent, Patent NO.: ZL201510803669.9
18. Peng L, Chenglin Z, Weigang Z et al (2019) Electric spindle device for rotary friction jointed equipment. Chinese Patent, Patent NO.: ZL201510155438.1
19. Zhang W, Li W, Zheng S et al (2019) Research on Motion Relationships and Transmission Efficiency of Planetary Roller Screw. The Proceedings of the 2018 Asia-Pacific International Symposium on Aero-space Technology (APISAT 2018). pp 2838–2848. https://doi.org/10.1007/978-981-13-3305-7_230
20. Brüßow H (2007) The evolution of eating systems. In: *The quest for food*. Springer, New York, pp 378–393. https://doi.org/10.1007/0-387-45461-6_4